PHYSICAL REVIEW E **73**, 010401(R) (2006)

Nonmonotonic fluctuation spectra of membranes pinned or tethered discretely to a substrate

Rolf-Jürgen Merath[1,2] and Udo Seifert[1]
[1]*II. Institut für Theoretische Physik, Universität Stuttgart, Pfaffenwaldring 57, 70550 Stuttgart, Germany*
[2]*Max-Planck-Institut für Metallforschung, Heisenbergstraße 3, 70569 Stuttgart, Germany*
(Received 23 September 2005; published 12 January 2006)

The thermal fluctuation spectrum of a fluid membrane coupled harmonically to a solid support by an array of tethers is calculated. For strong tethers, this spectrum exhibits nonmonotonic, anisotropic behavior with a relative maximum at a wavelength about twice the tether distance. The root-mean-square displacement is evaluated to estimate typical membrane displacements. Possible applications cover pillar-supported or polymer-tethered membranes.

DOI: 10.1103/PhysRevE.73.010401 PACS number(s): 82.70.−y, 87.16.Dg

INTRODUCTION

Thermal shape fluctuations of fluid membranes in the vicinity of a substrate depend both on the elasticity of the membrane and the specific type of interaction with the substrate [1]. For laterally homogeneous substrates the combination of steric, van der Waals, and electrostatic interactions determines the strength of these fluctuations. Such spectra, as measured experimentally using video microscopy [2,3], decrease with increasing wave vector since shorter wavelength fluctuations cost more bending energy. A qualitatively different type of interaction arises from tethering or pinning a membrane at discrete points to a substrate. By adjusting the length of the tethers the mean distance between substrate and membrane can be controlled. As tethering molecules, mostly thiolipids are used which consist of a lipid tail, a hydrophilic spacer (e.g., peptides [4,5] or polymers [6,7]), and a sulfur-based linker to the substrate. Likewise, end-functionalized membrane proteins can serve as tethers [8].

Micropatterned or nanopatterned substrates involving equidistant silicon pillars or gold dots have so far mainly been used to study the interaction with cell membranes [9] or an actin cortex [10], but similar experiments with vesicles should become possible as well. If the membrane binds specifically and firmly to these structures, it is effectively pinned at these points. For future biotechnological applications of such systems an understanding of how the thermal shape fluctuations are affected by tethering or pinning is of paramount interest.

In this paper, we determine the spectrum of shape fluctuations of such membranes. Surprisingly, we find a large range of parameters for which the fluctuations exhibit a nonmonotonic behavior with a maximum at a wavelength of the order of the tethering or pinning distance. Previous theoretical work on membrane conformations on structured substrates focused on groovelike or rough substrates [11,12], or vesicles adhering strongly to chemically patterned substrates [13]. In a formally related theoretical development, motivated by the red blood cell membrane, fluctuations of a fluid membrane coupling to the cytoskeleton were investigated [14–17].

THE MODEL

The membrane is linked at discrete points $\mathbf{r}_\alpha$ to a substrate by N springs as sketched in Fig. 1. The membrane surface is parameterized by a height profile $h(\mathbf{r})\equiv h(x,y)$ over a rectangular substrate of extensions L_x and L_y. The height $h(\mathbf{r})$ refers to the displacement with respect to the rest length l_0 of the tethers. The total energy functional

$$E \equiv \frac{\kappa}{2}\int_0^{L_x} \mathrm{d}x \int_0^{L_y} \mathrm{d}y [\nabla^2 h(\mathbf{r})]^2 + \sum_{\alpha=1}^{N} \frac{K_\alpha}{2} h^2(\mathbf{r}_\alpha) \qquad (1)$$

comprises membrane elasticity with bending rigidity κ and harmonic tethers with strength K_α. Assuming periodic boundary conditions in the lateral direction, a Fourier expansion of the height profile reads

$$h(\mathbf{r}) \equiv \sum_{\mathbf{k}} h_{\mathbf{k}} e^{i\mathbf{k}\cdot\mathbf{r}} \qquad (2)$$

with $\mathbf{k}\equiv(k_x,k_y)$ and $k_{x,y}=(0,\pm1,\pm2,\ldots)2\pi/L_{x,y}$. Since $h(\mathbf{r})$ is real, the complex Fourier coefficients obey $h_{-\mathbf{k}}=h_{\mathbf{k}}^*$. The spatial average of the height profile, $h_{\mathbf{0}}$, is real. The energy can be written as $E=\frac{1}{2}\Sigma_{\mathbf{k},\mathbf{k}'} h_{\mathbf{k}}^* D_{\mathbf{k},\mathbf{k}'} h_{\mathbf{k}'}$ with a nondiagonal coupling matrix $D_{\mathbf{k},\mathbf{k}'}$. Following a scheme introduced by Lin and Brown [17], a transformation to *independent* variables leads to

$$E = \mathbf{c}\cdot\mathbf{M}\mathbf{c} \equiv \sum_{r,r'} c_r M_{r,r'} c_{r'}. \qquad (3)$$

The components c_r (with $r=0, 1, 2, 3, \ldots$) of the vector $\mathbf{c}$ can be grouped into three sectors, $\mathbf{c}\equiv\left(\frac{1}{2}h_{\mathbf{0}},\{\mathrm{Re}\, h_{\mathbf{q}}\},\{\mathrm{Im}\, h_{\mathbf{q}}\}\right)$, where $\mathbf{q}$ runs through all independent, nonvanishing wave vectors. With the definitions

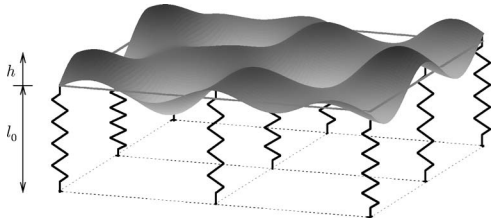

FIG. 1. Sketch of a membrane tethered to a substrate at discrete sites. A membrane conformation is characterized by the height profile $h(\mathbf{r})$, which denotes a displacement relative to the flat configuration at a height given by the rest length l_0 of the tethers.

$$E_r \equiv \begin{cases} 0 & \text{for } r=0 \\ \kappa L_x L_y |\mathbf{q}(r)|^4 & \text{for } r>0 \end{cases} \tag{4}$$

and

$$m_r^\alpha \equiv \begin{cases} \sqrt{2K_\alpha} & \text{for } r=0 \text{ (first sector)} \\ \sqrt{2K_\alpha}\cos[\mathbf{q}(r)\cdot\mathbf{r}_\alpha] & \text{for the second sector} \\ -\sqrt{2K_\alpha}\sin[\mathbf{q}(r)\cdot\mathbf{r}_\alpha] & \text{for the third sector} \end{cases} \tag{5}$$

the matrix $\mathbf{M}$ can be simplified to take the form

$$M_{r,r'} = E_r \delta_{r,r'} + \sum_{\alpha=1}^{N} m_r^\alpha m_{r'}^\alpha . \tag{6}$$

Since the energy (3) is quadratic, correlations are given by $\langle c_r c_{r'}\rangle = (k_B T/2) M^{-1}_{r,r'}$. The fluctuation spectrum $\langle |h_\mathbf{k}|^2\rangle$ can then be extracted from the (numerically calculated) inverse matrix $\mathbf{M}^{-1}$ via

$$\langle |h_\mathbf{k}|^2\rangle = \begin{cases} 2\ k_B T\ M^{-1}_{0,0} & \text{for } \mathbf{k}=\mathbf{0} \\ \frac{1}{2} k_B T (M^{-1}_{r(\mathbf{q},s=2),r(\mathbf{q},s=2)} + M^{-1}_{r(\mathbf{q},s=3),r(\mathbf{q},s=3)}) & \text{for } \mathbf{k}=\mathbf{q}, \end{cases} \tag{7}$$

where $r(\mathbf{q},s)$ is the index associated with the wave vector $\mathbf{q}$ and the sector index s [18].

Below we will compare the spectrum of the discretely tethered membrane with a simplified model called "continuous springs," where a membrane fluctuates in a laterally homogeneous harmonic potential of strength γ with energy functional

$$E^{(\gamma)} \equiv \frac{1}{2}\int_0^{L_x} \mathrm{d}x \int_0^{L_y} \mathrm{d}y \{\kappa[\nabla^2 h(\mathbf{r})]^2 + \gamma h^2(\mathbf{r})\}. \tag{8}$$

The fluctuation spectrum of this system reads

$$\langle |h_\mathbf{k}|^2\rangle^{(\gamma)} = \frac{k_B T}{L_x L_y (\kappa |\mathbf{k}|^4 + \gamma)}. \tag{9}$$

The overall strength of the discrete and the continuous springs is comparable for $\gamma = (1/L_x L_y)\Sigma_{\alpha=0}^N K_\alpha$, since these parameters lead to the same effective spring constant of the spring brush as a whole.

FLUCTUATION SPECTRA

We focus on a membrane attached to a *quadratic* array [21] of equally strong ($K_\alpha \equiv K$) equidistant tethers, with Δ as tether lattice constant, in the limit $L_{x,y} \to \infty$. First, the case of *pinning*, i. e., infinitely strong springs ($K \to \infty$), is analyzed. Dimensional analysis yields the spectrum in the form

$$\langle |h_\mathbf{k}|^2\rangle_{\text{pinned}} = \langle |h_\mathbf{0}|^2\rangle_{\text{pinned}} g(k_x\Delta, k_y\Delta), \tag{10}$$

with the amplitude at the origin ($\mathbf{k}=\mathbf{0}$) given by

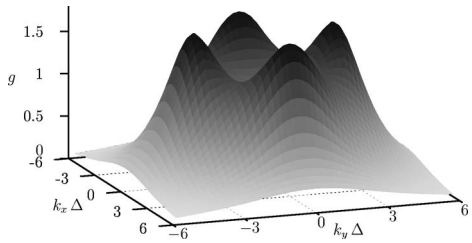

FIG. 2. The scaling function $g(k_x\Delta, k_y\Delta)$ of the fluctuation spectrum of a fluid membrane pinned by a quadratic array of infinitely strong springs. For quantitative data along the main axes of symmetry, see Fig. 3.

$$\langle |h_\mathbf{0}|^2\rangle_{\text{pinned}} = s \frac{k_B T}{\kappa N} \Delta^2 \tag{11}$$

and a numerically determined prefactor $s \simeq 3.9 \times 10^{-3}$. The scaling function $g(k_x\Delta, k_y\Delta)$ is shown in Fig. 2. The fourfold symmetry of the spectrum reflects the symmetry of the tether array. This spectrum is nonmonotonic with four relative maxima and four saddle points. The wavelength at the maxima is $\lambda_{\max} \simeq 1.11 \times 2\Delta$. Since undulation modes with a wavelength twice the distance Δ fulfill a pinning condition (i.e., no displacement at the site of the tethers), a naive guess would yield $\lambda_{\max} = 2\Delta$. For a quasi-one-dimensional system (with $k_y \equiv 0$) this would indeed be true [18]. However, for the full two-dimensional (2D) case, the interplay of all fluctuation modes apparent in the coupling matrix $\mathbf{M}$ (6) leads to deviations from this naive expectation towards a slightly larger wavelength.

From this spectrum, one can derive various one-dimensional spectra shown in Fig. 3. Cuts through the origin and a maximum, and through the origin and a saddle point, respectively, show the nonmonotonicity. The saddle point appears at a (by a factor of approximately $\sqrt{2}$) larger wavelength than the maxima, corresponding to the larger tether

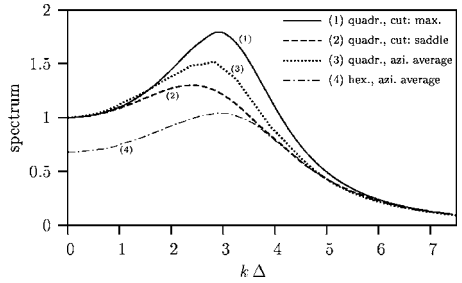

FIG. 3. One-dimensional plots of the universal 2D fluctuation spectrum $g(k_x\Delta, k_y\Delta)$ of a membrane pinned to a quadratic array of pinning sites (cf. Fig. 2). Cuts in two main directions, through a maximum (curve 1) and a saddle point (curve 2), of the 2D spectrum are shown and compared to an azimuthal average (curve 3). Curve 4 shows an azimuthal average of a spectrum for a *hexagonal* arrangement of pinning sites. The closer packed sites induce a sixfold symmetric 2D spectrum situated below the spectrum of the quadratic system. The constant s for the hexagonal pattern, $s^{(\text{hex.})} \simeq 2.5 \times 10^{-3}$, is different than in the quadratic case (11). For comparability, the hexagonal spectrum is divided by the prefactor $\langle |h_\mathbf{0}|^2\rangle_{\text{pinned}}$ of the quadratic case (10).

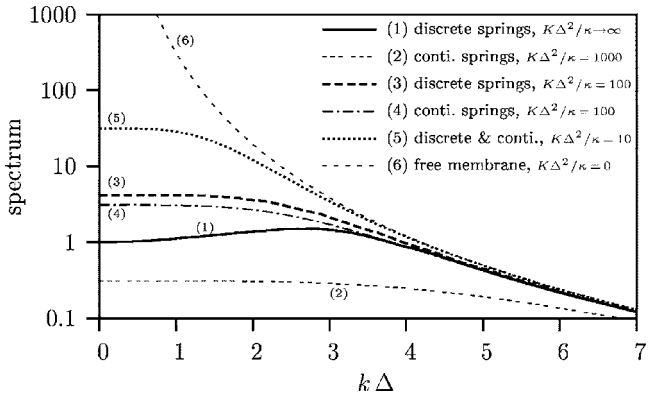

FIG. 4. The scaling function $f(K\Delta^2/\kappa,k_x\Delta,k_y\Delta)$ for the fluctuation spectrum of a quadratically tethered membrane for different spring stiffnesses (12). Azimuthal averages of the 2D spectra are compared to results from the continuous spring model (9). For comparision, the spectra for the continuous model are scaled by the prefactor $\langle|h_{\mathbf{0}}|^2\rangle_{\text{pinned}}$ of the discrete case. Curve 1 shows the azimuthal average of the 2D spectrum for pinning, i.e., infinitely strong springs. In the comparable continuous case ($\gamma\to\infty$), the spectrum vanishes. Curve 2 depicts the spectrum for strong continuous springs: while the "discrete spectrum" is still undistinguishable from curve 1, the "continuous spectrum" is located far underneath. Curves 3 and 4 give the corresponding discrete and continuous spectrum for moderately strong springs, respectively. For weaker springs the two cases yield nearly the same data shown in curve 5. The spectrum of a free membrane without tethers is shown as curve 6.

distance in this direction. Furthermore, the average of the 2D spectrum with respect to the azimuth angle is displayed. In the averaged spectrum, the wavelength of the maximum is $\lambda_{\text{max}}^{\text{azi}}\simeq 1.2\times 2\Delta$. It is larger than the wavelength corresponding to the relative maximum in the 2D spectrum but smaller than the wavelength corresponding to a saddle point.

For *finite spring constants K*, the fluctuation spectrum of a membrane tethered by a quadratic array can be expressed as

$$\langle|h_{\mathbf{k}}|^2\rangle = s\frac{k_BT}{\kappa N}\Delta^2 f(K\,\Delta^2/\kappa,k_x\Delta,k_y\Delta), \tag{12}$$

with a scaling function f that incorporates the spring elasticity. Since f is continuous and $f(\infty,k_x\Delta,k_y\Delta)=g(k_x\Delta,k_y\Delta)$, for sufficiently large spring constants K the nonmonotonicity of the spectrum persists. In Fig. 4, the wavelength dependence of the azimuthally averaged scaling function f is shown for different values of $K\Delta^2/\kappa$ and compared to the spectrum (9) of a continuous confining harmonic potential. For weak springs, a tethered membrane behaves like a membrane with continuous confinement. For moderately strong spring constants, deviations from the continuous spectrum occur, with the spectrum of the discrete tethering being systematically larger than the continuous one. The positions of the relative maxima in the 2D spectra depend on $K\Delta^2/\kappa$. For infinitely strong springs the maximum of the spectrum reaches its lowest possible wavelength. For decreasing spring constants the wavelength corresponding to the relative maxima increases. Finally, below a critical value of the spring constant, $K\Delta^2/\kappa|_{\text{crit}}\simeq 100$, the relative maxima disappear and the spectrum decays monotonically.

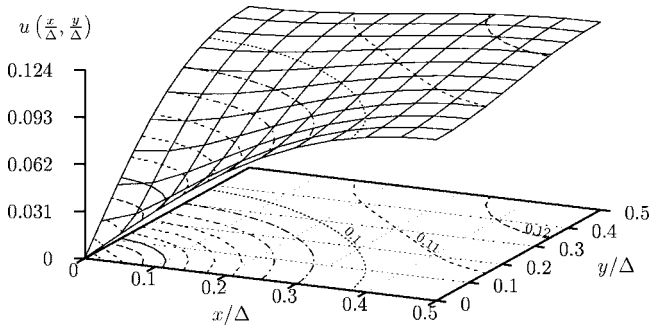

FIG. 5. Scaling function $u(x/\Delta,y/\Delta)$ for the RMSD, $\sqrt{\langle h^2(\mathbf{r})\rangle}$, of a membrane pinned at a quadratic array of sites. Due to symmetry only one quarter of a unit cell is shown. Contour lines are drawn in steps of 0.01.

A nonmonotonic fluctuation spectrum (and hence a negative effective surface tension) was first noted by Gov and Safran (GS) for the model of a fluid membrane under the influence of a sinusoidal confining potential [16]. The nonmonotonicity appears there only for weak potentials, whereas it only exists for strong potentials in our model. Moreover, the spectral maximum in the GS model occurs at a significantly larger wavelength (compared to the periodicity of the potential) than in our model. In addition to the fluctuation spectrum obtainable with both methods, the correlations $\langle h_{\mathbf{k}}h_{\mathbf{k}'}\rangle$—and thus the real-space fluctuations $\langle h^2(\mathbf{r})\rangle$—for a nontranslational invariant system (i.e., with fixed pinning sites) are directly accessible in our approach.

REAL-SPACE FLUCTUATIONS

We now determine the average width of the membrane in real space. The height profile can be written as $h(\mathbf{r})=2\mathbf{w}(\mathbf{r})\cdot\mathbf{c}$ with [17] $\mathbf{w}(\mathbf{r})\equiv[1,\{\cos(\mathbf{q}\cdot\mathbf{r})\},\{-\sin(\mathbf{q}\cdot\mathbf{r})\}]$. Given the inverse matrix $\mathbf{M}^{-1}$ and applying $\langle c_r c_{r'}\rangle=(k_BT/2)M^{-1}_{r,r'}$, the mean-square displacement reads

$$\langle h^2(\mathbf{r})\rangle = 2\,k_BT\sum_{r,r'} w_r(\mathbf{r})M^{-1}_{r,r'}w_{r'}(\mathbf{r}). \tag{13}$$

Typical membrane elongations are represented by the root-mean-square displacement (RMSD) $\sqrt{\langle h^2(\mathbf{r})\rangle}$. Only if the maximum of this RMSD is significantly smaller than the rest length of the springs, can this model be trusted quantitatively since it does not yet include the steric hindrance by the substrate. The maximum of the RMSD is a measure to estimate how far above a substrate the membrane has to be placed in order to avoid undesirable contact or adhesion of the bilayer to the substrate.

For *pinning* ($K\to\infty$), we find

$$\sqrt{\langle h^2(\mathbf{r})\rangle}_{\text{pinned}} \equiv \sqrt{k_BT/\kappa}\Delta\; u(x/\Delta,y/\Delta) \tag{14}$$

with a scaling function $u(x/\Delta,y/\Delta)$ shown in Fig. 5. The maximum of the RMSD in the pinned case occurs in the center of a unit cell and is given by

$$\max\{\sqrt{\langle h^2(\mathbf{r})\rangle}\}_{\text{pinned}} \equiv p\sqrt{k_BT/\kappa}\Delta \tag{15}$$

with a constant $p \simeq 0.124$.

For *finite* spring constants K, the maximum of the RMSD takes the form

$$\max\{\sqrt{\langle h^2(\mathbf{r})\rangle}\} \equiv p\sqrt{k_BT/\kappa}\Delta\ w(K\Delta^2/\kappa) \tag{16}$$

with a scaling function w. For weak springs, $w(K\Delta^2/\kappa)$ approaches $1/(p\sqrt{8})(K\Delta^2/\kappa)^{-1/4}$, which follows from the known result $\langle h^2(\mathbf{r})\rangle^{(\gamma)} = k_BT/(8\sqrt{\kappa\gamma})$ for a membrane bound in a harmonic potential [19]. For strong springs, w approaches 1. The crossover between these two scaling limits occurs around $K\Delta^2/\kappa = (p\sqrt{8})^{-4} \simeq 66.1$, where the two asymptotes intersect.

SUMMARIZING PERSPECTIVE

Discrete tethering of a membrane to a substrate has a profound implication on the fluctuation spectrum. For strong enough tethers, this spectrum becomes nonmonotonic with a maximum determined by the spacing of the tethers. An interpretation of such a spectrum in terms of a continuous model would require a term $-|\sigma|(\nabla h)^2$ in (8) implying a negative "surface tension." For sufficiently weak tethers, however, the discrete tethering can indeed be replaced by a continuous harmonic confining potential. The explicit introduction of an additional regular (positive) surface tension, e.g., caused by the area constraint of a vesicle whose bound part is considered [20], into the energy (1) of our model poses no problems.

Our quantitative data on the mean displacements caused by these fluctuations should provide valuable hints for the experimentalists on how large the rest length l_0 of the pillars and tethers has to be in order to avoid contact with the substrate. For a smaller l_0, one should include a direct interaction with the substrate, which could be attractive due to van der Waals interaction, and/or repulsive, due to steric interactions. In either case one could include an effective potential $V(h)$ to the energy functional. Its minimization will then lead to a laterally inhomogeneous "ground-state" profile $l_0(\mathbf{r})$ as in studies of membrane adhesion to structured substrates [12]. In another extension of our model one can study the fluctuation of two almost parallel membranes connected by polymeric linkers. The fluctuation of the relative distance between the membranes, i.e., the peristaltic mode, is then governed by an effective Hamiltonian (1) and will show the nonmonotonic behavior for strong enough linkers as well.

[1] For a review, see U. Seifert, Adv. Phys. **46**, 13 (1997).
[2] A. Zilker, H. Engelhardt, and E. Sackmann, J. Phys. (Paris) **48**, 2139 (1987).
[3] J. O. Rädler *et al.*, Phys. Rev. E **51**, 4526 (1995).
[4] R. Naumann *et al.*, Langmuir **19**, 5435 (2003).
[5] N. Bunjes *et al.*, Langmuir **13**, 6188 (1997).
[6] A. Förtig *et al.*, Macromol. Symp. **210**, 329 (2003).
[7] O. Purrucker *et al.*, ChemPhysChem **5**, 327 (2004).
[8] F. Giess *et al.*, Biophys. J. **87**, 3213 (2004).
[9] J. P. Spatz, ChemPhysChem **5**, 383 (2004).
[10] W. H. Roos *et al.*, ChemPhysChem **4**, 872 (2003).
[11] P. S. Swain and D. Andelman, Langmuir **15**, 8902 (1999).
[12] P. S. Swain and D. Andelman, Phys. Rev. E **63**, 051911 (2001).
[13] R. Lipowsky *et al.*, J. Phys.: Condens. Matter **17** S537 (2005).
[14] N. Gov, A. G. Zilman, and S. Safran, Phys. Rev. Lett. **90**, 228101 (2003).
[15] J.-B. Fournier, D. Lacoste, and E. Raphaël, Phys. Rev. Lett. **92**, 018102 (2004).
[16] N. Gov and S. A. Safran, Phys. Rev. E **69**, 011101 (2004).
[17] L. C.-L. Lin and F. L. H. Brown, Biophys. J. **86**, 764 (2004).
[18] R.-J. Merath, Diploma thesis, Universität Stuttgart, 2004 (unpublished).
[19] S. A. Safran, "*Statistical Thermodynamics of Surfaces, Interfaces and Membranes*, Frontiers in Physics, Vol. 90 (Addison-Wesley, Reading, MA, 1994).
[20] U. Seifert, Phys. Rev. Lett. **74**, 5060 (1995).
[21] A hexagonal array leads to qualitatively similar results—up to the different symmetry [18].